

## Effect of glycerol on the morphology of nanocomposites made from thermoplastic starch and starch nanocrystals

Nancy L. García<sup>a,b</sup>, Laura Ribba<sup>a</sup>, Alain Dufresne<sup>c</sup>, Mirta Aranguren<sup>d</sup>, Silvia Goyanes<sup>a,\*</sup>

<sup>a</sup> Laboratorio de Polímeros y Materiales Compuestos, Dep. De Física, FCEN – UBA and IFIBA-CONICET, Ciudad Universitaria, C1428EGA, Pabellón 1, Intendente Güiraldes 2160, Ciudad Autónoma de Buenos Aires, Argentina

<sup>b</sup> Universidad Nacional de San Martín (UNSAM), Campus Miguelete, San Martín, Prov. De Buenos Aires, Argentina

<sup>c</sup> The International School of Paper, Print Media and Biomaterials (Pagora), Grenoble Institute of Technology, BP 65, 38402 Saint Martin d'Hères Cedex, France

<sup>d</sup> INTEMA, Av. Juan B. Justo 4302 7608FDQ, Mar del Plata, Argentina

### ARTICLE INFO

#### Article history:

Received 2 June 2010

Received in revised form 8 November 2010

Accepted 11 November 2010

Available online 19 November 2010

#### Keywords:

Biodegradable  
Nanocomposites  
Starch  
Nanocrystals  
Waxy maize  
Glycerol

### ABSTRACT

Fully bio-based nanocomposites were prepared using starch nanoparticles obtained by acidic hydrolysis of waxy maize starch granules as reinforcement. The same type of starch, which contains 99 wt.% amylopectin, was used to prepare glycerol plasticized and unplasticized matrices. The X-ray diffraction pattern of the plasticized reinforced materials displays both A and B-type peaks, showing that the crystalline structure of the nanocrystals was not affected by processing. The storage modulus of the composite material increases, with respect to the unfilled film, by 470% at 50 °C, while the permeability increases by 70%. This is probably due to a good association of glycerol with the nanoparticles leading to a fibrillar structure, studied by scanning electron microscopy of plasticized and unplasticized composites.

© 2010 Elsevier Ltd. All rights reserved.

### 1. Introduction

Petrochemical based polymers predominate in many applications such as packaging of foods due to their easy processing, excellent barrier properties and low cost. However, there is currently an increasing interest in replacing conventional synthetic polymers by more sustainable materials. The permanent search for materials to delay the imminent shortage of petrochemical resources has become more intense, driving the development of new biopolymers obtained from renewable resources. The packaging industry dependence on non-renewable fossil resources will clearly be reduced considerably, in accordance with international trends of caring for the environment.

In this context, starch is a promising material because of its versatility, low price and availability. It is a semi-crystalline polymer stored in the form of granules as reserve in most plants, and composed of repeating 1,4- $\alpha$ -D glucopyranosyl units: amylose and amylopectin. The amylose is an almost linear polymer, in which the repeating units are linked by  $\alpha$  (1–4) linkages; the amylopectin has  $\alpha$  (1–4)-linked backbone and ca. 5% of  $\alpha$  (1–6)-linked branches. The ratio of amylose to amylopectin depends upon the plant source. For

waxy maize starch, the amount of amylopectin is approximately 99 wt.%. (Thomas & Atwell, 1997)

Starch has received considerable attention as a biodegradable thermoplastic polymer. It is not truly thermoplastic but can be converted into a continuous polymeric entangled phase by mixing with enough water or plasticizer (generally polyols, such as glycerol). The resulting material can be manufactured using technology already developed for the production of synthetic plastics, thus representing a minor investment. However, the hydrophilic nature of thermoplastic starches makes them susceptible to moisture attack with the resultant changes in dimensional stability and mechanical properties. In addition, retrogradation and crystallization of the mobile starch chains lead to undesired variations of its thermo-mechanical properties. In fact several properties change with the type of starch used (García, Famá, Dufresne, Aranguren, & Goyanes, 2009); the manufacturing process (Flores, Famá, Rojas, Goyanes, & Gerschenson, 2007); and aging, (Famá, Goyanes, & Gerschenson, 2007).

Tailored improved properties can be obtained by adding fillers into thermoplastic starch, preserving its biodegradability in the case of biodegradable fillers. For example, Chillo et al. (Chillo, Flores, Mastromatteo, Conte, Gerschenson, & Del Nobile, 2008) worked in chitosan/starch composite films, and showed that the tensile strength value increases with increasing chitosan concentrations, but the effect on the elongation at break results negligible. Simi-

\* Corresponding author. Tel.: +54 11 45763300; fax: +54 11 45763357.  
E-mail address: [goyanes@df.uba.ar](mailto:goyanes@df.uba.ar) (S. Goyanes).

lar behavior was reported by Famá, Bittante, Sobral, Goyanes, and Gerschenson (2010), in wheat bran/starch composite films. The composites show an important improvement in the storage modulus and hardening keeping elongation at break as high as 70%.

However, the presence of other biodegradable fillers such as garlic powder (Famá et al., 2010) or Nisin (Imran, El-Fahmy, Revol-Junelles, & Desobry, 2010), usually incorporated into the matrix as antimicrobial agents, leads to detriments in the tensile strength and elastic modulus values and to an increase of the strain to break.

Promising fillers are polysaccharide nanocrystals, where the nano-sized fillers can impart enhanced mechanical and barrier properties. Following this strategy, nanocomposite materials have been prepared from plasticized starch reinforced with cellulose microfibrils (Dufresne, Dupeyre, & Vignon, 2000; Dufresne, & Vignon, 1998; Kumar & Singh, 2008; Martins, Magina, Oliveira, Freire, Silvestre, Neto, & Gandini, 2009), cellulose nanocrystals (Anglès & Dufresne, 2000, 2001; Chang, Jian, Zhen, Yu, & Ma, 2010; Mathew & Dufresne, 2002; Mathew, Thielemans, & Dufresne, 2008; Teixeira, Pasquini, Curvelo, Corradini, Belgacem, & Dufresne, 2009), or starch nanocrystals (Angellier, Molina-Boisseau, Dole, & Dufresne, 2006; Viguié, Molina-Boisseau, & Dufresne, 2007; Garcia, Ribba, Dufresne, Aranguren, & Goyanes, 2009; Kristo & Biliaderis, 2007). In the case of the work of Angellier et al. (2006), the authors limited the study to the reinforcing properties of waxy maize starch nanocrystals (tensile tests, DMA) with filler content between 0 and 15 wt.%. In a later work, Garcia et al. (2009), using another kind of matrix (cassava starch) showed that the addition of nanocrystals not only improved the mechanical properties but also reduced the water vapor permeability by 40%.

These systems are complex and composed of amorphous and semi-crystalline starch domains, polysaccharide filler, main plasticizer – glycerol – and water, interacting competitively. From the above discussed investigations, it appears that one of the main issues determining the final properties of the materials is the location of the main plasticizer within these systems, which is very difficult to control. In a recent work, García et al. (2009), have shown, employing glycerol as plasticizer in biofilms based on waxy maize and cassava starches, that the glycerol produces stronger interactions with the cassava starch than with the waxy starch matrix. This feature has a major effect on most of the properties of the ensuing composites.

The main objective of the present work was to investigate the effect of a low content (2.5 wt.%) of starch nanocrystals obtained by acid hydrolysis of waxy maize starch granules in a glycerol plasticized waxy maize starch matrix. Mechanical properties and permeability were characterized, and the results were explained in terms of the localization of glycerol in the sample. The results of both characterizations are essential when using these materials in the packaging industry. The mechanical properties when handling the material and the permeability since the diffusing humidity from or towards the content will change its organoleptic properties or/and change its sensitivity to microbial attack. To explain the results, samples without glycerol were prepared and compared in terms of their thermal degradation and fracture morphology.

## 2. Experimental

### 2.1. Materials

Waxy maize starch (N-200) as a white powder, was kindly provided by Roquette Freres S.A. (Lestree, France). Glycerol (J.T. Baker, 99% purity) and sulfuric acid (J.T. Baker) were purchased from Interchemistry S.A., Argentina.

### 2.2. Preparation of starch nanocrystals

Waxy maize starch nanocrystals were obtained according to a previously described method (Angellier, Choisnard, Molina-Boisseau, Ozil, & Dufresne, 2004). Briefly, acidic hydrolysis of 36.725 g of waxy maize starch granules was performed in a 250 ml 3.16 M H<sub>2</sub>SO<sub>4</sub> solution, at 40 °C and 100 rpm. The mixture was subjected to an orbital shaking action during 5 days. Subsequently, the ensuing insoluble residue was washed with distilled water and separated by successive centrifugations at 10,000 rpm and 5 °C, until neutrality. The aqueous suspensions of starch nanoparticles were stored at 4 °C after adding several drops of chloroform.

### 2.3. Preparation of plasticized and unplasticized films

Thermoplastic starch was processed by casting a mixture of waxy maize starch granules, glycerol and distilled water. A quantity of 10 g of starch and 5 g of glycerol as plasticizer was dispersed in 185 g of distilled water (the weight percentages, wt.%, relative to the dry total mass (starch + plasticizer) are 66.6 wt.% of starch and 33.3 wt.% of glycerol. Similar amounts were used in previous work (Famá, Rojas, Goyanes, & Gerschenson, 2005; Famá, Flores, Gerschenson, & Goyanes, 2006; Famá et al., 2007, 2010; Flores, Haedo, Campos, & Gerschenson, 2007; Flores, Famá et al., 2007). The mixture was heated from room temperature at a heating rate of 1.59 °C min<sup>-1</sup> under mechanical stirring during 28 min until gelatinization, which occurred at ~70 °C. After gelatinization, the gel was degassed for 30 min under vacuum mechanical pumping, according to Famá et al. (2005), and García, Ribba, Dufresne, Aranguren, and Goyanes, 2009). The nanocomposite films were prepared by adding the aqueous suspension of waxy maize starch nanocrystals in the desired quantity (2.5 wt.% relative to the dry total mass, starch + plasticizer + nanocrystals). Then, the mixture was stirred for 10 min at 250 rpm and degassed for 1 more hour. The ensuing mixture was cast in a plastic mold and evaporated in a ventilated oven at 50 °C for 48 h. Solid films having a thickness between 200 and 300 μm were obtained. Matrix and composite films were stored at 43% relative humidity (RH) (K<sub>2</sub>CO<sub>3</sub> saturated solution) for two weeks before characterization and testing. It is worth mentioning that due to the high content of glycerol, it would be inappropriate to work with the films conditioned at high relative humidity, since they would not have the appropriate characteristics.

Unplasticized samples, unfilled and composite containing 2.5 wt.% of nanocrystals, were prepared and stored in the same way as plasticized samples.

### 2.4. Characterization

#### 2.4.1. Transmission electron microscopy (TEM)

Transmission electron micrographs of starch nanocrystals were taken with an EM 301 Philips transmission electron microscope using an acceleration voltage of 60 kV. A dilute starch nanocrystals suspension was sonicated during 10 min. After sonication, a drop of the starch nanocrystals suspension was deposited onto a carbon-coated microscopy grid and negatively stained with an aqueous 2% solution of uranyl acetate during 1 min. The liquid in excess was blotted with filter paper and the remaining liquid was dried before the specimen observation.

#### 2.4.2. Field emission scanning electron microscopy (FE-SEM)

A SEM with Field Emission Gun (FEG) Zeiss DSM982 GEMINI was used to examine the morphology of starch nanoparticles, a drop of the starch nanocrystals suspension was deposited onto a carbon-coated microscopy grid. The cryogenic fractured surfaces of films were also examined. In this last case, the samples were coated with a thin sputtered gold layer before analysis.

#### 2.4.3. Dynamic mechanical analysis (DMA)

Dynamic mechanical measurements were performed for the matrix and composite, using a Dynamic Mechanical Thermal Analyzer (DMTA IV) Rheometric Scientific equipment working in the rectangular tension mode at 1 Hz, in the temperature range between  $-120$  and  $70$  °C, at a heating rate of  $2$  °C  $\text{min}^{-1}$ . The dimensions of the samples were  $25$  mm  $\times$   $9$  mm  $\times$   $0.4$  mm. The samples were subjected to a cyclic strain lower than  $0.04\%$ . This strain value was sufficiently low to insure that the mechanical response of the specimen was within its linear viscoelastic range. The set up allowed determining the storage modulus  $E'$ , the loss modulus  $E''$  and the ratio of these two parameters,  $\tan \delta = E''/E'$

#### 2.4.4. Water vapor permeability (WVP)

WVP tests were conducted using ASTM E96-00 (1996). Film specimens were conditioned for two weeks in desiccators at  $25$  °C and  $43\%$  RH (equilibrium with a  $\text{K}_2\text{CO}_3$  saturated solution) before being analyzed. Each film sample was sealed over a circular opening of  $21.85$  mm in diameter in a permeation cell that was stored at  $25$  °C in desiccators. To maintain a  $58\%$  RH gradient across the film, silica gel ( $0\%$  RH), activated at  $200$  °C, was placed inside the cell and a sodium bromide (NaBr) saturated solution ( $58\%$  RH) was placed in the desiccators, outside the cell. Water vapor transport was determined from the weight gain of the permeation cell. After reaching the steady state condition (about  $2$  h), eight weight measurements were made over the first  $24$  h, followed by one measurement per day during ten days. Changes in the weight of the cell were recorded to the nearest  $0.0001$  g and plotted as a function of time for  $10$  days. Cells were carefully shaken horizontally after every weighing. The slope of each line was calculated by linear regression ( $R^2 > 0.99$ ) and the rate of water vapor transfer (WVT,  $\text{g h}^{-1} \text{m}^{-2}$ ) was determined from the slope of the straight line ( $\text{g h}^{-1}$ ) divided by the cell area ( $\text{m}^2$ ). The thickness of each film was measured with a microscope at six randomly selected points after the permeation test. Three replicate samples were analyzed. The WVP was calculated as:

$$\text{WVP} = \frac{\text{WVT}}{S(R1 - R2)} \times T \quad (1)$$

where  $S$  is the saturation vapor pressure of water at the test temperature ( $25$  °C),  $R1$  is the relative humidity in the desiccators,  $R2$  is the relative humidity inside the permeation cell, and  $T$  is the film thickness.

#### 2.4.5. Attenuated total reflectance Fourier transform infrared spectroscopy (ATR/FTIR)

Absorbance spectrum of the starch-based films were recorded on a Nicolet 8700 Fourier transform infrared spectrometer using the single reflection horizontal attenuated total reflectance (ATR) accessory Smart Orbit, with diamond crystal at an incident angle of  $45^\circ$ . The spectra were obtained with a resolution of  $4 \text{ cm}^{-1}$  as the average of  $64$  scans.

#### 2.4.6. X-ray diffraction

Matrix and composite films were submitted to X-ray radiation using a diffractometer Philips, model PW 1510 with a vertical goniometer operating at Cu  $\text{K}\alpha$  radiation wavelength ( $\lambda = 1.542$  Å),  $40$  kV,  $30$  mA and sampling interval of  $0.02^\circ$ . Scattered radiation was detected in the angular range  $10$ – $35^\circ$  ( $2\theta$ ).

#### 2.4.7. Thermogravimetric analysis (TGA)

Thermogravimetric analysis was carried out for both the matrix and the composite, using a Perkin–Elmer TGA-50H instrument under nitrogen atmosphere at  $30 \text{ ml min}^{-1}$  and at a heating rate of  $5$  °C  $\text{min}^{-1}$ . The temperature scan was run from room temperature to  $500$  °C.

### 3. Results and discussions

#### 3.1. Characterization of waxy maize starch nanocrystals

Fig. 1a shows TEM micrographs of waxy maize starch nanoparticles. TEM observations were performed using a drop of a suspension of nanocrystals in water that was previously sonicated.

The morphology of the nanocrystals is similar to the one reported in our previous study (García et al., 2009) and also by others authors (Chen, Cao, Chang, & Huneault, 2008; Namazi & Dadkhah, 2010). The primary nanoparticles have an average size below  $50$  nm and form aggregates of around  $1$   $\mu\text{m}$ . These aggregates result from the high density of OH groups inherent to any polysaccharidic material and present in the surface of individual nanocrystals. The nanoparticles display therefore a high tendency to strongly associate with each other by hydrogen bonding forces.

Fig. 1b shows a FE-SEM micrograph of a drop of starch nanocrystals suspension. It is observed that the nanocrystals form an associated structure of individual crystalline lamellae looking like a kind of “bouquet”. This architecture is similar to the observations of Oostergetel and van Bruggen (1993), who proposed a helix organization in form of clusters as well as Capron, Robert, Colonna, Brogly, and Planchot (2007). Similar structures were observed by Waigh, Kato, Donald, Gidley, Clarke, and Riekell (2000).

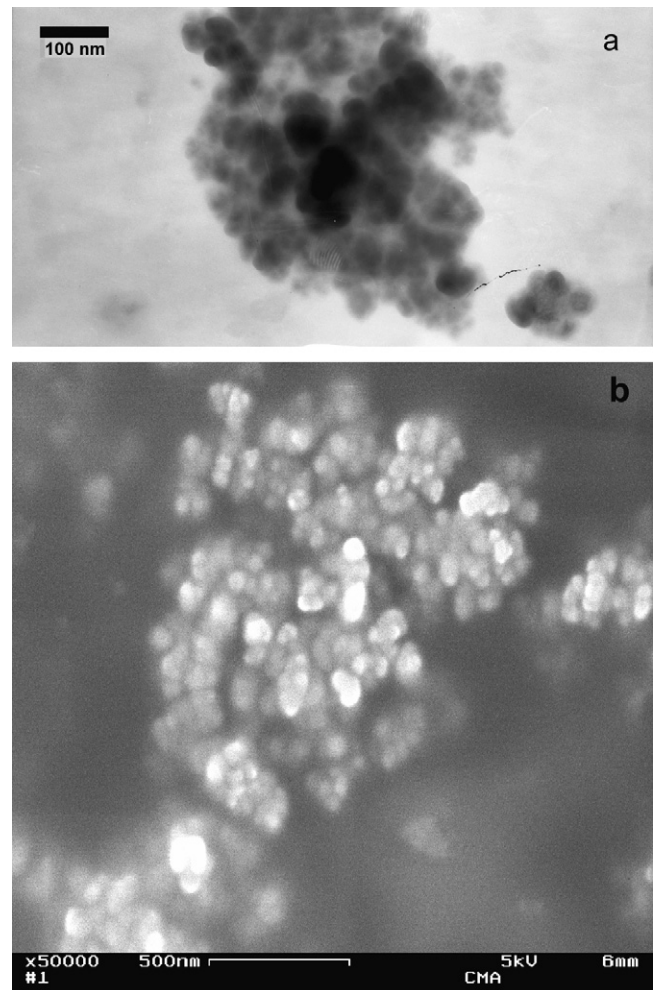


**Fig. 1.** (a) Transmission electron micrographs of a dilute suspension of waxy maize starch. (b) Scanning electron micrographs (FE-SEM) of a dilute suspension of waxy maize starch nanocrystals.

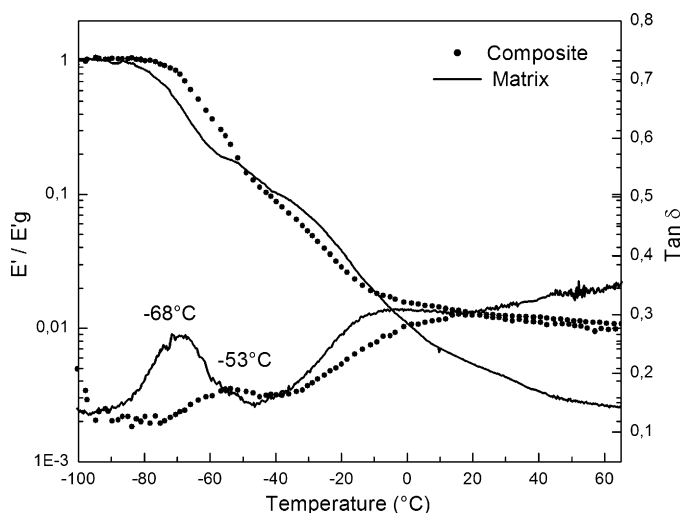


**Fig. 2.** Isochronal evolution of the logarithm of the relative storage modulus and tangent of the phase angle at 1 Hz as a function of temperature for the glycerol plasticized starch matrix and related nanocomposite reinforced with 2.5 wt.% waxy maize starch nanocrystals.

### 3.2. Characterization of glycerol plasticized and unplasticized films

As indicated in Section 2, both glycerol plasticized and unplasticized starch matrices and related nanocomposites reinforced with 2.5 wt.% starch nanocrystals were prepared. Films were characterized through different techniques (DMA, WVP, X-ray diffraction and TGA), although unfortunately, unplasticized films were too brittle to allow measurements with various of these methods.

#### 3.2.1. Dynamic mechanical analysis (DMA)

Fig. 2 presents the isochronal evolution (1 Hz) of both the logarithm of the relative storage modulus ( $E'/E'g$ ), defined as the ratio between the actual modulus and the modulus in the glassy state, and the tangent of the phase angle  $\tan \delta$ , as a function of temperature. Measurements were performed for the glycerol plasticized starch matrix and related composite reinforced with 2.5 wt.% of starch nanocrystals.

The evolution of  $\tan \delta$  (solid line for the matrix and filled circles for the composite in Fig. 2) with temperature displays two relaxation processes. These two relaxations occur in the temperature range where the modulus drops, and are representative of the heterogeneous nature of the glycerol plasticized starch system, an already well-known feature. The low temperature relaxation process is ascribed to the main relaxation associated with the glass transition of glycerol-rich domains whereas the high temperature relaxation corresponds to starch-rich domains, as already reported (De Menezes, Siqueira, Curvelo, & Dufresne, 2009; Forsell, Mikkilä, Moates, & Parker, 1997).

Globally, adding starch nanocrystals induces a shift towards higher temperatures, a broadening and a magnitude decrease of the two relaxation processes. In particular, in the present study, the shift of the main relaxation of the glycerol-rich phase is significant (from  $-68^\circ\text{C}$  to  $-53^\circ\text{C}$ ) when adding only 2.5 wt.% starch nanocrystals. It is an indication that starch nanocrystals are much more compatible with the glycerol-rich phase than with the waxy maize starch-rich phase, therefore it is suggested that the filler was mainly located in the glycerol-rich domains of the matrix, in agreement with Anglès and Dufresne (2001), where a migration of the main plasticizer from the amylopectin-rich domains towards the filler/matrix interface was observed in plasticized starch tunicin whiskers nanocomposites. Also the broadening of

the relaxation is probably induced by a wide distribution of friction mechanisms.

Clearly, the type of starch used as the matrix has a remarkable effect on the morphology and corresponding phase relaxations. Thus, in a previous research focused on starch nanocrystals reinforced-cassava starch films plasticized with glycerol, it was shown an almost negligible increase of the low temperature relaxation process associated with a relocation of glycerol induced by specific interactions between the filler and the main plasticizer (García et al., 2009).

Regarding the logarithm of the relative storage modulus, the most important feature is the significant reinforcing effect observed in the rubbery state of the matrix by addition of just 2.5 wt.% nanocrystals. Indeed, the modulus drop through  $T_g$  is much more significant for the unfilled matrix (nearly three decades) than for composite (around two decades). At  $50^\circ\text{C}$ , the storage rubbery modulus of the nanocomposite film reinforced with 2.5 wt.% starch nanocrystals is roughly 470% higher than the one of the unfilled matrix.

#### 3.2.2. Morphological characterization by SEM

Figs. 3 and 4 show micrographs of the cryo-fractured surfaces of glycerol plasticized and unplasticized composite films, respectively, containing 2.5 wt.% nanocrystals.

By comparing both sets of composites, a completely different aspect is observed. The unplasticized sample (Fig. 5) displays a rather smooth homogeneous surface associated with a brittle fracture. For the plasticized composite specimen (Fig. 4), a nanometric fibrillar structure is observed. It will be referred as starch "nanothreads" afterwards. As shown in Fig. 3, these nanothreads appear throughout the whole fractured surface. Since they are not observed in the filled unplasticized starch material (Fig. 5), these structures must be associated to the presence of glycerol. From DMA experiments, a close association of starch nanocrystals with glycerol-rich domains in the matrix was suspected. It is proposed to ascribe the nanothread structure to nanoparticles included in glycerol-rich domains. Probably, the high level of glycerol used (50% related to starch) increased the phase separation and was responsible for the higher interaction of glycerol with nanocrystals.

It was recently shown by Angellier-Coussy, Putaux, Molina-Boisseau, Dufresne, Bertoft, and Perez (2009), that acid hydrolysis of waxy maize starch resulted in a population of branched and linear dextrans. It was reported that nanocrystals correspond to crystalline lamellae present in native starch granules and that between 150 and 300 double-helical components are making up these crystalline domains. We therefore suspect that the fibrillar structure observed in Fig. 3 results from the association of aggregated nanocrystals through glycerol. It seems that glycerol wraps or covers aggregates of nanocrystals, and acts promoting the growth of the starch nanothreads. Besides, according to the proposed by Anglès and Dufresne (2001) in a composite cellulose/starch, the amylopectin of the starch matrix can crystallize on the surface of the nanocrystals due to the accumulation of plasticizers (glycerol and water) in this region. Then, it is proposed that the nanothreads are formed by the nanocrystals, glycerol and transcrystallized amylopectine

#### 3.2.3. Water vapor permeability (WVP)

The WVP values measured were  $(3.8 \pm 0.3) \times 10^{-10} \text{ g s}^{-1} \text{ m}^{-1} \text{ Pa}^{-1}$  for the unfilled plasticized film, and  $(6.8 \pm 0.1) \times 10^{-10} \text{ g s}^{-1} \text{ m}^{-1} \text{ Pa}^{-1}$  for the plasticized film reinforced with 2.5% of nanocrystals. It can be seen that the permeability to water vapor increases (by 79%) upon the addition of only 2.5 wt.% waxy maize starch nanocrystals. This result is opposite to the one obtained using a cassava starch matrix (García et al., 2009) and in natural rubber films (Angellier, Molina-Boisseau, Lebrun, & Dufresne, 2005), where the nanocrystals were well distributed,

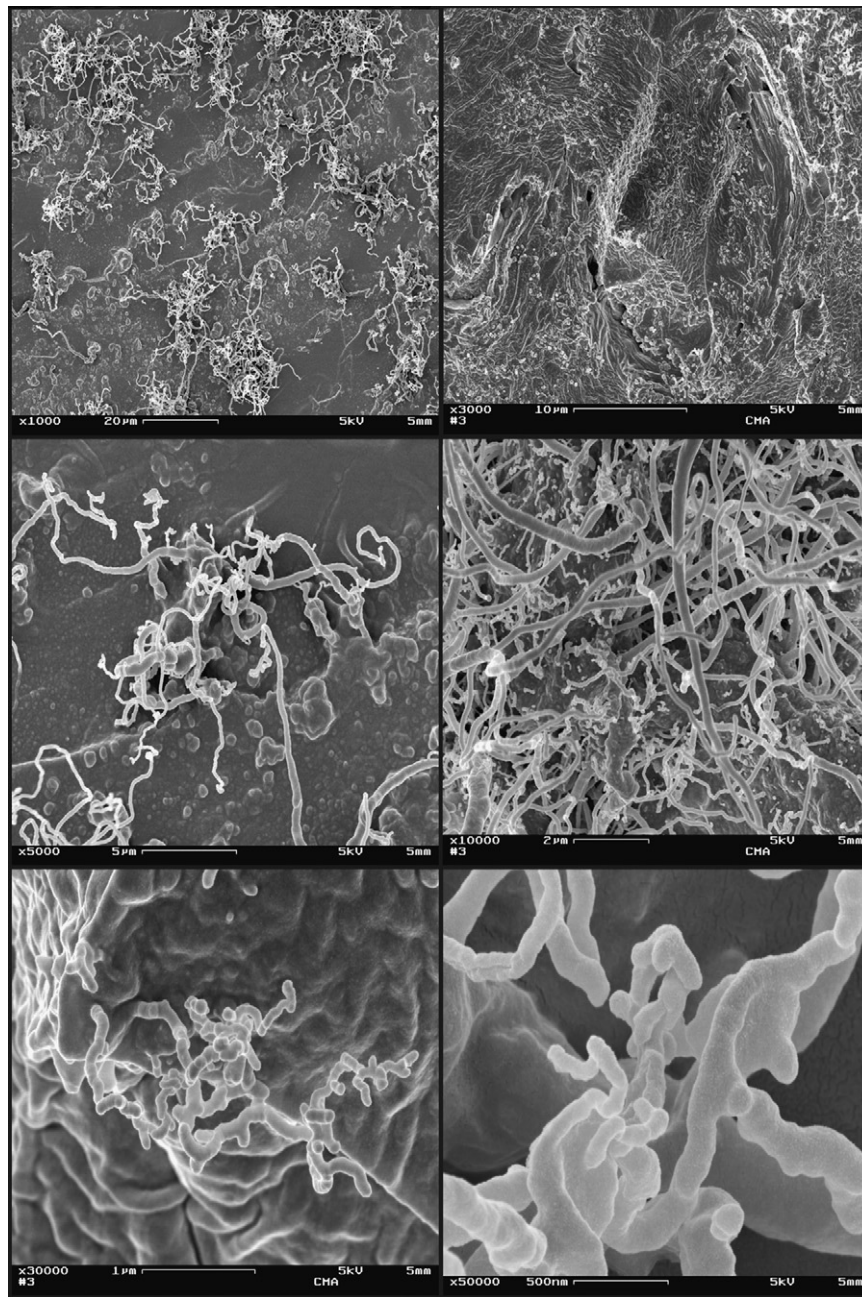


**Fig. 3.** Scanning electron micrographs from the fractured surface of glycerol plasticized composite film containing 2.5 wt.% nanocrystals.

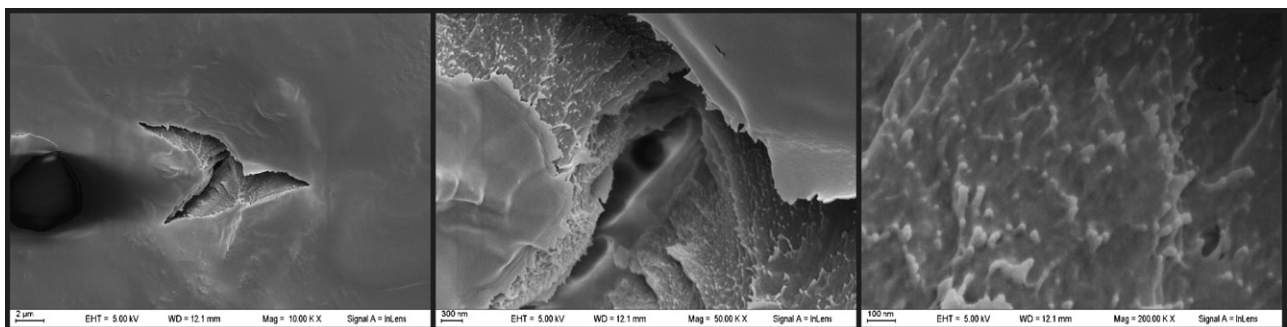


**Fig. 4.** Scanning electron micrographs from the fractured surface of unplasticized composite film containing 2.5 wt.% nanocrystals.

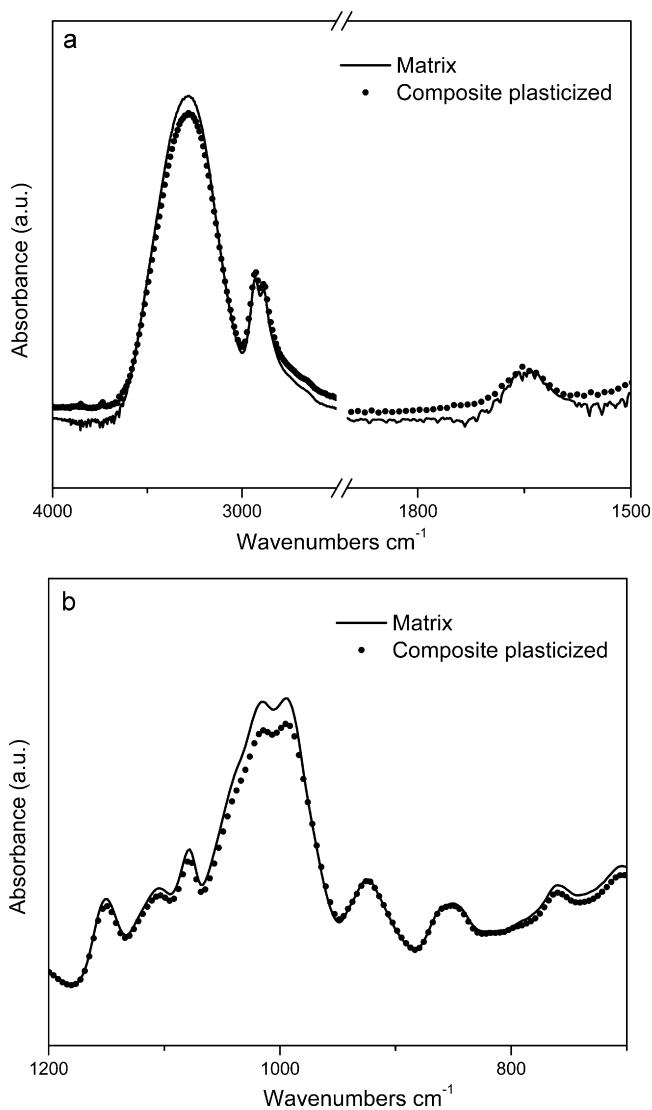


**Fig. 5.** Infrared spectra in the spectral (a) 4000–1500  $\text{cm}^{-1}$  and (b) 1500–700  $\text{cm}^{-1}$  region for glycerol plasticized starch matrix and related nanocomposite reinforced with 2.5 wt.% waxy maize starch nanocrystals.

generating a tortuous path for the water vapor diffusion and consequently inducing a decrease of the permeability of the films to both water vapor and oxygen. On the contrary, in this case the nanocrystals are glue–glycerol bonded, forming threads with high concentration of OH and thus, forming a preferential path for water vapor diffusion through the nanothreads, which clearly increases the permeability of the film.

### 3.2.4. Attenuated total reflectance Fourier transform infrared spectroscopy (ATR/FTIR)

Fig. 5a and b show the FTIR spectra obtained for the glycerol plasticized waxy maize starch sample and related composite reinforced with 2.5 wt.% starch nanocrystals in the 4000–1500  $\text{cm}^{-1}$  and 1500–700  $\text{cm}^{-1}$  region, respectively. No significant difference was observed between both specimens in the two FTIR spectral regions. The short-range order defined as the double helical conformation and revealed by the ratio of the 995/1022  $\text{cm}^{-1}$  did not vary contrarily to what was reported for glycerol plasticized cassava starch reinforced with starch nanocrystals by García et al. (2009).

Fig. 6 shows the FTIR spectra of the unplasticized waxy maize starch film (matrix) and related composite reinforced with 2.5 wt.% nanocrystals in the wavenumber range 1300–700  $\text{cm}^{-1}$ . Again,

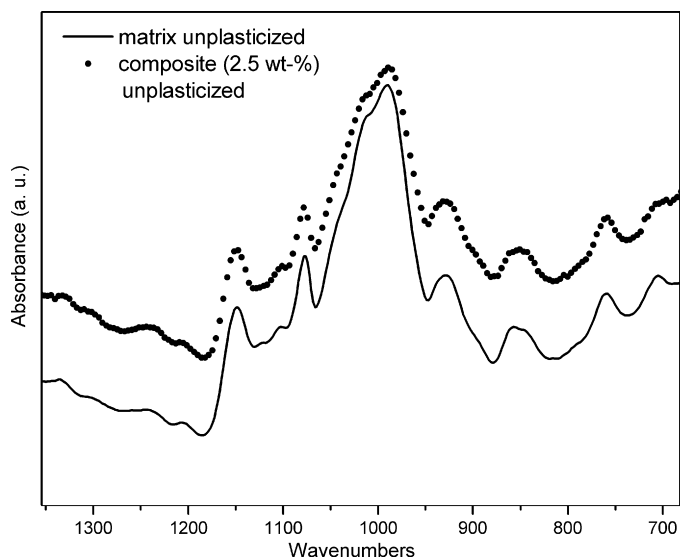


**Fig. 6.** Infrared spectra in the spectral 1300–700  $\text{cm}^{-1}$  region for unplasticized starch matrix and related nanocomposite reinforced with 2.5 wt.% waxy maize starch nanocrystals.

the neat unplasticized starch and composite films display similar features in the whole FTIR spectral range. However, comparing the spectra in the region around 1000  $\text{cm}^{-1}$  for unplasticized and glycerol plasticized composite, it is revealed that the ratio of the 995/1022  $\text{cm}^{-1}$  peaks is significantly higher for the unplasticized sample, driving from a nematic to a smectic structure as proposed by Capron et al. (2007). Nanocrystals aggregates contribute to the local order only in the presence of glycerol. These observations confirm the close association of starch nanocrystals with glycerol and their helicoidal structure organization.

### 3.2.5. X-ray diffraction

X-ray diffraction was used to observe potential changes in the crystallinity of the waxy maize starch matrix upon addition of 2.5 wt.% nanocrystals. The patterns obtained for both films, the matrix and the composite, are shown in Fig. 7. Experiments were performed in the interval 4–30° ( $2\theta$ ), identifying the most intense

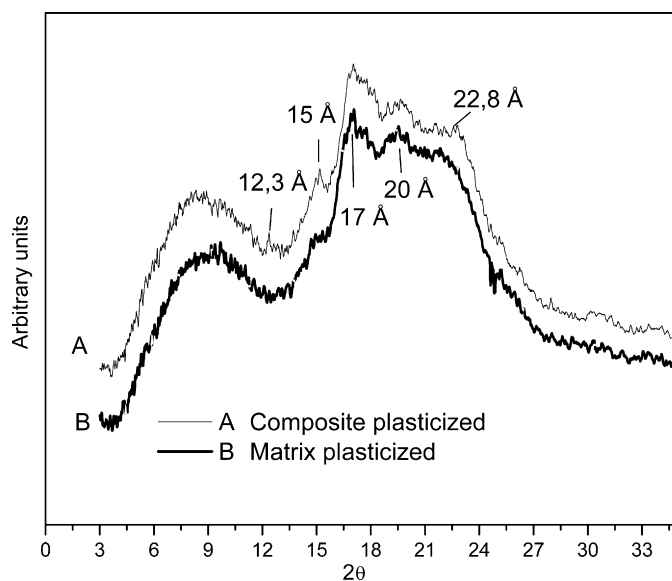


**Fig. 7.** X-ray diffraction patterns for glycerol plasticized starch matrix and related nanocomposite reinforced with 2.5 wt.% waxy maize starch nanocrystals.

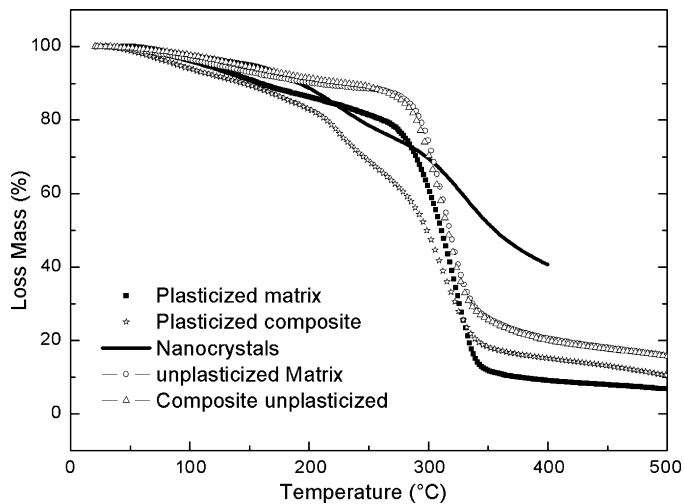


**Fig. 8.** TGA for glycerol plasticized starch matrix and related nanocomposite reinforced with 2.5 wt.% waxy maize starch nanocrystals. The curve corresponding to starch nanocrystals has been added as reference.

peaks and calculating the distances between crystalline planes,  $d$  (Å), from the diffraction angles ( $^\circ$ ) according to Bragg's law:  $n\lambda = 2d \sin \theta$ ; where  $\lambda$  is the wavelength of the X-ray beam and  $n$  the order of reflection. Both films display typical diffraction peaks of B-type crystalline structure, with peaks at  $2\theta = 17^\circ$  and  $20^\circ$ , corresponding to  $d$  spacing of 5.2 Å and 4.4 Å, respectively. The peaks at  $5.6^\circ$ ,  $22^\circ$  and  $24^\circ$  ( $d$  spacing of 15.8 Å, 4 Å and 3.7 Å) are hardly noticeable. For the nanocomposite film, additional diffraction peaks characteristic of the A-type allomorph are detected, even if the starch nanocrystal content is low. Peaks around  $15^\circ$ ,  $17$ – $18^\circ$  and  $23^\circ$  are observed.

### 3.2.6. Thermogravimetric analyses TGA

Thermogravimetric analysis (TGA) measurements were carried out to access the thermal stability of glycerol plasticized waxy maize starch with and without starch nanocrystals. Results are shown in Fig. 8. The thermal decomposition of the starchy matrix occurs in three main steps, as reported in the literature (Jiang, Qiao, & Sun, 2006; Rajan, Prasad, & Abraham, 2006; Rath & Singh, 1998; Wilhelm, Sierakowski, Souza, & Wypych, 2003). The first stage corresponds to the loss of water and low-molecular-weight compounds. The second stage is due to the decomposition of the glycerol-rich phase and nanocrystals (the TGA curve obtained for freeze-dried nanocrystals was used as reference, solid line in Fig. 8), and the third stage corresponds to the oxidation of the partially decomposed starch (Wilhelm et al., 2003). The mass drop associated with the loss of water is much lower for nanocrystals compared to other samples because of the freeze-drying.

A significant mass loss (around 36%) is observed for the plasticized composite film in the temperature range 80–280 °C. It is ascribed to the decomposition of nanocrystals and glycerol, which is expected to degrade above 180 °C (Cyras, Tolosa Zenklusen, & Vazquez, 2006), since the nanocrystal and glycerol content represents 2.5% and 33% of the total mass, respectively. The lower thermal stability reported for the composite could be ascribed to a closer association of glycerol with starch nanoparticles. This more marked heterogeneous nature for composites probably leads to the two-step mass drop observed in Fig. 8.

In addition, during acid hydrolysis via sulfuric acid, acidic sulfate ester groups are likely formed on the nanoparticle surface. It was shown for cellulose nanocrystals that even at low levels, the ensuing sulfate groups caused a significant decrease in degradation temperature and an increase in char fraction confirming that the sulfate groups act as flame retardants (Roman &

Winter, 2004). A similar phenomenon probably occurs with starch nanocrystals.

TGA curves obtained for the unplastified starch matrix and related composite are also included in Fig. 8. Contrarily to glycerol plasticized samples, the two curves superimpose almost perfectly. The effect of the addition of starch nanoparticles in the unplastified matrix is negligible compared to the one induced in the glycerol plasticized material.

## 4. Conclusions

Starch nanoparticles were prepared by acid hydrolysis of waxy maize starch granules. They were used to reinforce a waxy maize starch matrix obtained by gelatinization. Both unfilled and filled, as well as unplastified and glycerol plasticized films were processed by the casting/evaporation technique. The structure of crystalline nanoparticles was not affected by the processing method. All the results lead to the conclusion that a close association exists between starch nanocrystals and glycerol-rich domains. This association was supported by SEM, from a peculiar fibrillar morphology for glycerol plasticized composite, and by DMA, from a strong alteration of the relaxation process assigned to the glass transition of glycerol-rich domains. These changes result in an unexpected increase of the water vapor permeability of the plasticized film upon addition of starch nanoparticles.

## Acknowledgments

The authors thank the financial support from the Universidad de Buenos Aires (UBACyT X094), Consejo Nacional de Investigaciones Científicas y Técnicas de la República Argentina (PIP 11220090100699 and PIP 6250-05, Agencia Nacional de Investigaciones Científicas y Tecnológicas de la República (PICT Raíces 2006-02153) Argentina and Scientific program of Cooperation between the Ministry of Science, Technology and Productive Innovation of the Argentine Republic (MINCYT) and ECOS-Sud program (no. A08E02).

## References

- Angellier, H., Choinsard, L., Molina-Boisseau, S., Ozil, P., & Dufresne, A. (2004). Optimization of the preparation of aqueous suspensions of waxy maize starch nanocrystals using a response surface methodology. *Biomacromolecules*, 5, 1545–1551.
- Angellier, H., Molina-Boisseau, S., Dole, P., & Dufresne, A. (2006). Thermoplastic starch–waxy maize starch nanocrystals nanocomposites. *Biomacromolecules*, 7, 531–539.
- Angellier, H., Molina-Boisseau, S., Lebrun, L., & Dufresne, A. (2005). Processing and structural properties of waxy maize starch nanocrystals reinforced natural rubber. *Macromolecules*, 38, 3783–3792.
- Angellier-Coussy, H., Putaux, J., Molina-Boisseau, S., Dufresne, A., Bertoff, E., & Perez, S. (2009). The molecular structure of waxy maize starch nanocrystals. *Carbohydrate Research*, 17, 1558–1566.
- Anglès, M. N., & Dufresne, A. (2000). Plasticized starch/tunicin whiskers nanocomposites: 1. Structural analysis. *Macromolecules*, 33, 8344–8353.
- Anglès, M. N., & Dufresne, A. (2001). Plasticized starch/tunicin whiskers nanocomposites: 2 Mechanical behavior. *Macromolecules*, 34, 2921–2931.
- STM E96-00. (1996). *Standard test methods for water vapor transmission of materials*. Annual book of ASTM. Philadelphia, PA: American Society for Testing and Materials.
- Capron, I., Robert, P., Colonna, P., Brogly, & Planchot, M. V. (2007). Starch in rubbery and glassy states by FTIR spectroscopy. *Carbohydrate Polymers*, 68, 249–259.
- Chang, P. R., Jian, R., Zheng, P., Yu, J., & Ma, X. (2010). Preparation and properties of glycerol plasticized-starch (GPS)/cellulose nanoparticle (CN) composites. *Carbohydrate Polymers*, 79, 301–305.
- Chen, Y., Cao, X., Chang, P. R., & Huneault, M. A. (2008). Comparative study on the films of poly (vinyl alcohol)/pea starch nanocrystals and poly (vinyl alcohol)/native pea starch. *Carbohydrate Polymers*, 73, 8–17.
- Chillo, S., Flores, S., Mastromatteo, M., Conte, A., Gerschenson, L., & Del Nobile, M. A. (2008). Influence of glycerol and chitosan on tapioca starch-based edible film properties. *Journal of Food Engineering*, 88, 159–168.
- Cyras, V. P., Tolosa Zenklusen, M. C., & Vazquez, A. (2006). Relationship between structure and properties of modified potato starch biodegradable films. *Journal of Applied Polymer Science*, 101, 4313–4319.

- De Menezes, A. J., Siqueira, G., Curvelo, A. A. S., & Dufresne, A. (2009). Extrusion and characterization of functionalized cellulose whiskers reinforced polyethylene nanocomposites. *Polymer*, *50*, 4552–4563.
- Dufresne, A., Dupeyre, D., & Vignon, M. R. (2000). Cellulose microfibrils from potato cells: Processing and characterization of starch/cellulose microfibrils composites. *Journal of Applied Polymer Science*, *76*, 2080–2092.
- Dufresne, A., & Vignon, M. R. (1998). Improvement of starch films performances using cellulose microfibrils. *Macromolecules*, *31*, 2693–2696.
- Famá, L., Bittante, A. M. B. Q., Sobral, P. J. A., Goyanes, S., & Gerschenson, L. N. (2010). Garlic powder and wheat bran as fillers: Their effect on the physico-chemical properties of edible biocomposites. *Materials Science and Engineering: C*, *30*, 853–859.
- Famá, L., Flores, S. K., Gerschenson, L., & Goyanes, S. (2006). Physical characterization of cassava starch biofilms with special reference to dynamic mechanical properties at low temperatures. *Carbohydrate Polymers*, *66*, 8–15.
- Famá, L., Goyanes, S., & Gerschenson, L. (2007). Influence of storage time at room temperature on the physicochemical properties of cassava starch films. *Carbohydrate Polymers*, *70*, 265–273.
- Famá, L., Rojas, A. M., Goyanes, S., & Gerschenson, L. (2005). Mechanical properties of tapioca-starch edible films containing sorbates. *LWT*, *38*, 631–639.
- Flores, S., Famá, L., Rojas, A. M., Goyanes, S., & Gerschenson, L. (2007). Physical properties of tapioca-starch edible films: Influence of filmmaking and potassium sorbate. *Food Research International*, *40*, 257–265.
- Flores, S., Haedo, A. S., Campos, C., & Gerschenson, L. (2007). Antimicrobial performance of potassium sorbate supported in tapioca starch edible films. *European Food Research and Technology*, *225*, 375–384.
- Forsell, P. M., Mikkilä, J. M., Moates, G. K., & Parker, R. (1997). Phase and glass transition behavior of concentrated barley starch–glycerol–water mixtures, a model for thermoplastic starch. *Carbohydrate Polymers*, *34*, 275–282.
- García, N. L., Famá, L., Dufresne, A., Aranguren, M., & Goyanes, S. (2009). A comparison between the physico-chemical properties of tuber and cereal starches. *Food Research International*, *42*, 976–982.
- García, N. L., Ribba, L., Dufresne, A., Aranguren, M., & Goyanes, S. (2009). Physico mechanical properties of biodegradable starch nanocomposites. *Macromolecular Materials and Engineering*, *294*, 169–177.
- Imran, M., El-Fahmy, S., Revol-Junelles, A., & Desobry, S. (2010). Cellulose derivative based active coatings: Effects of nisin and plasticizer on physico-chemical and antimicrobial properties of hydroxypropyl methylcellulose films. *Carbohydrate Polymers*, *81*, 219–225.
- Jiang, W., Qiao, X., & Sun, K. (2006). Mechanical and thermal properties of thermoplastic acetylated starch/poly (ethylene-co-vinyl alcohol) blends. *Carbohydrate Polymers*, *65*, 139–143.
- Kristo, E., & Biliaderis, C. G. (2007). Physical properties of starch nanocrystal-reinforced pullulan films. *Carbohydrate Polymers*, *68*, 146–158.
- Kumar, A. P., & Singh, R. P. (2008). Biocomposites of cellulose reinforced starch: Improvement of properties by photo-induced crosslinking. *Bioresource Technology*, *99*, 8803–8809.
- Martins, I. M. G., Magina, S. P., Oliveira, L., Freire, C. S. R., Silvestre, A. J. D., Neto, C. P., et al. (2009). New biocomposites based on thermoplastic starch and bacterial cellulose. *Composites Science and Technology*, *69*, 2163–2168.
- Mathew, A. P., & Dufresne, A. (2002). Morphological investigation of nanocomposites from sorbitol plasticized starch and tunicin whiskers. *Biomacromolecules*, *3*, 609–617.
- Mathew, A. P., Thielemans, W., & Dufresne, A. (2008). A mechanical properties of nanocomposites from sorbitol plasticized starch and tunicin whiskers. *Journal of Applied Polymer Science*, *109*, 4065–4074.
- Namazi, H., & Dadkhah, A. (2010). Convenient method for preparation of hydrophobically modified starch nanocrystals with using fatty acids. *Carbohydrate Polymers*, *79*, 731–737.
- Oostergetel, G. T., & van Bruggen, E. F. J. (1993). The crystalline domains in potato starch granules are arranged in a helical fashion. *Carbohydrate Polymers*, *21*, 7–12.
- Rajan, A., Prasad, V. S., & Abraham, T. E. (2006). Enzymatic esterification of starch using recovered coconut oil. *International Journal of Biological Macromolecules*, *39*, 265–272.
- Rath, S. K., & Singh, R. P. (1998). On the characterization of grafted and ungrafted starch, amylose, and amylopectin. *Journal of Applied Polymer Science*, *70*, 1795–1810.
- Roman, M., & Winter, W. T. (2004). Effect of sulfate groups from sulfuric acid hydrolysis on the thermal degradation behavior of bacterial cellulose. *Biomacromolecules*, *5*, 1671–1677.
- Teixeira, E. M., Pasquini, D., Curvelo, A. A. S., Corradini, E., Belgacem, M. N., & Dufresne, A. (2009). Cassava bagasse whiskers reinforced plasticized cassava starch. *Carbohydrate Polymers*, *78*, 422–431.
- Thomas, D. J., & Atwell, W. A. (1997). *Starches*. St. Paul: Eagan Press Handbook Series.
- Viguié, J., Molina-Boisseau, S., & Dufresne, A. (2007). Processing and characterization of waxy maize starch films plasticized by sorbitol and reinforced with starch nanocrystals. *Macromolecular Bioscience*, *7*, 1206–1216.
- Waigh, T. A., Kato, K. L., Donald, A. M., Gidley, M. J., Clarke, C. J., & Riekkel, C. (2000). Side-chain liquid-crystalline model for starch. *Starch*, *52*, 450–460.
- Wilhelm, H. M., Sierakowski, M. R., Souza, G. P., & Wypych, F. (2003). Starch films reinforced with mineral clay. *Carbohydrate Polymers*, *52*, 101–110.